



Published in final edited form as:

Curr Biol. 2013 December 2; 23(23): 2423–2429. doi:10.1016/j.cub.2013.10.023.

Antagonistic spindle motors and MAPs regulate metaphase spindle length and chromosome segregation

Viktoriya Syrovaktina^{1,*}, Chuanhai Fu^{1,2,*}, and Phong T. Tran^{1,3}

¹Cell & Developmental Biology, University of Pennsylvania, Philadelphia, PA 19104 USA

²Department of Biochemistry, University of Hong Kong, Hong Kong

³Institut Curie, CNRS UMR144, Paris 75005, France

Abstract

Metaphase describes a phase of mitosis where chromosomes are attached and oriented on the bipolar spindle for subsequent segregation at anaphase. In diverse cell types, the metaphase spindle is maintained at characteristic constant length [1–3]. Metaphase spindle length is proposed to be regulated by a balance of pushing and pulling forces generated by distinct sets of spindle microtubules (MTs) and their interactions with motors and MT-associated proteins (MAPs). Spindle length is further proposed to be important for chromosome segregation fidelity, as cells with shorter or longer than normal metaphase spindles, generated through deletion or inhibition of individual mitotic motors or MAPs, showed chromosome segregation defects. To test the force-balance model of spindle length control and its effect on chromosome segregation, we applied fast microfluidic temperature-control with live-cell imaging to monitor the effect of deleting or switching off different combinations of antagonistic force contributors in the fission yeast metaphase spindle. We show that spindle midzone proteins kinesin-5 cut7p and MT bundler ase1p contribute to outward pushing forces, and spindle kinetochore proteins kinesin-8 klp5/6p and dam1p contribute to inward pulling forces. Removing these proteins individually led to aberrant metaphase spindle length and chromosome segregation defects. Removing these proteins in antagonistic combination rescued the defective spindle length and, in some combinations, also partially rescued chromosome segregation defects.

Results and Discussion

In diverse cell types, the metaphase spindle maintains a characteristic steady-state constant length [1–3], which is thought to be important for ensuring correct chromosome-to-MT attachment prior to anaphase. It is proposed that a balance of antagonistic forces produced by motors and MAPs located at the spindle midzone, the kinetochore, and/or astral MTs is required to maintain the constant metaphase spindle length [1–3]. However, the force-

Correspondence: tranp@mail.med.upenn.edu.

*These authors contributed equally to this work

Publisher's Disclaimer: This is a PDF file of an unedited manuscript that has been accepted for publication. As a service to our customers we are providing this early version of the manuscript. The manuscript will undergo copyediting, typesetting, and review of the resulting proof before it is published in its final citable form. Please note that during the production process errors may be discovered which could affect the content, and all legal disclaimers that apply to the journal pertain.

balance model has never been tested in a live-cell manner. In rare occasions of removal of antagonistic forces, e.g., double-deletion of antagonistic motors, the metaphase spindle length appeared rescued [4–7], but its subsequent effect on chromosome segregation was not known.

We present here a live-cell study using the simple fission yeast *Schizosaccharomyces pombe*, combined with fast microfluidic temperature-control for inactivating thermo-sensitive genes, effectively tuning protein functions on-off rapidly during mitosis, to directly test the force-balance model and determine its consequences on chromosome segregation. Fission yeast exhibits all the phases of mitosis identical to that of mammalian cells [8]. However, unlike mammalian cells, the number of motors and MAPs implicated in spindle dynamics in fission yeast are fewer [9]. Thus, mechanisms of fission yeast spindle length regulation may be viewed as “core” conserved mechanisms through evolution.

Motors and MAPs control the steady-state constant metaphase spindle length

We reasoned that forces contributing to the metaphase spindle length maintenance would come from motors and MAPs [1–3]. To define a set of antagonistic motors and MAPs regulating spindle length, we performed a targeted deletion or inactivation screen of the fission yeast motors and selective MAPs known to have spindle length defects. We used the degradation of cyclin B (*cdc13p*-GFP) as a proxy for metaphase to anaphase transition (Fig. 1A) [10, 11], and defined the final metaphase spindle length as the length immediately before the disappearance of *cdc13p*-GFP from the spindle. Our screen identified the kinetochore proteins: heterodimer kinesin-8 *klp5/6p* and the MT coupler *dam1p* as the major contributors to the inward pulling force on the spindle, as their individual deletion resulted in longer metaphase spindles compared to wildtype (Fig. 1B), consistent with previous findings [12, 13]. Kinesin-8 *klp5/6p* is a MT plus end depolymerase which converts MT depolymerization to cargo movement [14, 15]. Similarly, *dam1p* is a MAP which binds processively to MT and converts MT depolymerization to cargo movement [16, 17]. Thus, *Klp5/6p* can be viewed as an active force transducer, and *dam1p* can be viewed as a passive force transducers, both converting MT depolymerization into the inward pulling force experienced by the spindle. We also identified the spindle midzone bundler MAP *ase1p* as the major contributor to the outward pushing force on the spindle, as its deletion resulted in shorter metaphase spindles compared to wildtype (Fig. 1B), consistent with previous findings [18, 19]. As a MT bundler of defined angular polarity [20], *ase1p* can be viewed as a force resistor, resisting the inward force due to *klp5/6p* and *dam1p*. Finally, kinesin-14 *pk11p* also appeared to play a major role in spindle length control, as its deletion resulted in shorter metaphase spindles compared to wildtype (Fig. 1B). However, its reported localization at the spindle pole body [7], and its role in focusing MTs at the spindle poles [21, 22], suggests that it does not directly contribute to the pulling or pushing forces for spindle length control, but instead plays a role in spindle formation itself. In deed, we observed high frequency of MT protrusions from the spindle poles in *pk11* cells, ~50% of spindles have protrusion in *pk11* cells, compared to zero in wildtype cells (Fig. S1A, S1B), indicative of spindle mal-formation. We thus exclude *pk11p* from the current analysis. While numerous motors and MAPs have been reported to play a role in metaphase spindle length regulation [4, 6], for clarity, we focus on the motors and MAPs which have the strongest

measurable defects in spindle lengths, and which localize only to the kinetochores or the spindle midzone.

Kinesin-5 cut7p is reported to play a role in biopolar spindle formation, by organizing and sliding apart antiparallel MTs from opposite poles [23]. cut7p is essential and a conditional temperature-sensitive strain was isolated previously [23]. We used a microfluidic fast temperature-control device created in our lab [24], to inactivate the temperature-sensitive cut7.24^{ts} strain precisely at metaphase (Fig. 1C). Upon inactivation of cut7p at the non-permissive 35°C, the metaphase spindle immediately shortened until the spindle became a focused monopolar structure (Fig. 1C). This is consistent with cut7p being the major contributor to the outward pushing force. Thus, cut7p can be viewed as an active force producer, sliding interpolar MTs apart as the outward pushing force experienced by the spindle.

Interestingly, in *C. elegans* and mammalian somatic cells, kinesin-5 Eg5 is not needed for the maintenance of metaphase spindle length [25–27]. In mammals, highly dynamic interpolar MTs can compensate for the absence of Eg5 [28]; and in *C. elegans*, the relatively more robust astral MTs compared to the smaller interpolar MTs, can produce pulling force on the spindle and compensate for the absence of Eg5 [27]. In comparison, fission yeast has no astral MTs during metaphase, and does not have highly dynamic and robust interpolar MTs. Therefore, cut7p becomes indispensable for spindle length maintenance in fission yeast.

We next monitored spindle elongation dynamics to determine how the new steady-state spindle length is achieved. As inactivation of cut7p shortened completely the metaphase spindle (Fig. 1C, 2A), we examined the *ase1*⁻, *klp6*⁻, and *dam1*⁻ mutants. The spindle of wildtype cells typically elongates at 0.23 ± 0.02 $\mu\text{m}/\text{min}$ during prophase to reach a steady-state metaphase length of 3.10 ± 0.34 μm , with duration of prophase-metaphase of 22 ± 5 min (Fig. 1D, 1E, 1F, S1C, S1D). In contrast, *ase1*⁻ elongates at 0.10 ± 0.03 $\mu\text{m}/\text{min}$, has metaphase length of 1.82 ± 0.33 μm , and prophase-metaphase duration of 28 ± 3 min; *klp6*⁻ elongates at 0.32 ± 0.04 $\mu\text{m}/\text{min}$, has metaphase length of 6.33 ± 1.60 μm , and prophase-metaphase duration of 38 ± 11 min; and *dam1*⁻ elongates at 0.21 ± 0.07 $\mu\text{m}/\text{min}$, has metaphase length of 4.41 ± 1.62 μm , and prophase-metaphase duration of 52 ± 13 min (Fig. 1D, 1E, 1F, S1C, S1D).

We stress that changes in spindle length is likely due primarily to the force contributors, and not to the activation of the spindle assembly checkpoint (SAC) [29–32], which would be expected to prolong the prophase-metaphase duration and lead to changes in spindle length. In the absence of *mad2p*, a major SAC protein monitoring kinetochore-to-MT attachment [29–32], metaphase spindle lengths in the double deletions *klp5*⁻:*mad2*⁻ and *dam1*⁻:*mad2*⁻ remained similar to that of *klp5*⁻ and *dam1*⁻ alone, respectively (Fig. S1E); while the prophase-metaphase duration of the double-mutants is similar to that of wildtype (Fig. S1F). We conclude that, consistent with the force-balance model, removing individual contributors of force results in enhanced antagonistic effect from the remaining force contributors, which leads to a new steady-state metaphase spindle length.

Removal of antagonistic spindle forces can rescue metaphase spindle length defects

Pushing and pulling can be viewed as antagonistic forces controlling the steady-state metaphase spindle length. To test if removal of antagonist force contributors can restore or rescue the metaphase spindle length to that of wildtype, we observed metaphase spindle length upon deletion and/or inactivation of antagonistic force contributors. As shown, inactivation of *cut7p* at 35°C with the fast microfluidic temperature-control device led to an immediate decrease in metaphase spindle length (Fig. 1C, 2A). The decrease is relatively quick, occurring over durations of ~4–6 min (Fig. 2A). The quick spindle shrinkage is the result of the inactivation of *cut7.24^{ts}* while both *klp5/6p* and *dam1p* are still present. In the *klp6* cells, where metaphase spindles are longer than wildtype due to the removal of the inward pulling force contributor *klp6p* (Fig. 1B, 2B), inactivation of *cut7p* did not immediately lead to spindle shrinkage (Fig. 2B). Instead, the majority of the *cut7.24^{ts}:klp6* spindles slowly decreased in length over the 10-min observation duration, and some even maintained the same length or slightly increased in length (Fig. 2B). Our interpretation is that in the absence of *klp6*, *dam1p* is still at the kinetochore to capture MTs. Further, *dam1p* is passive, waiting for a MT depolymerization event to manifest the pulling force [16, 17]. If no MT depolymerization occurs, no pulling force would be possible, resulting in no spindle length decrease or even in an increase in spindle length in the short-term (~5 min duration). In the long-term, all MTs will tend to depolymerize and *dam1p* would then act to pull the spindle inward slowly [16, 17]. A similarly slow spindle length decrease is also observed in the *dam1* cells when *cut7p* is inactivated (Fig. 2C). However, all *cut7.24^{ts}:dam1* spindles showed persistent slow spindle length decrease. Our interpretation is that in the absence of *dam1*, *klp6p* at the kinetochore can still capture MTs and persistently promote MT depolymerization, resulting in sustained slow spindle shrinkage [14, 15]. Thus, force-balance is a tug-of-war between *cut7p* and *ase1p* against *klp5/6p* and *dam1p*. This model predicts that the triple removal of *cut7p*, *klp5/6p*, and *dam1p* would remove both inward and outward forces, leading to a static constant-length metaphase spindle. The double-deletion *dam1 :klp5* is lethal [33]. However, the temperature-sensitive double-mutant *dam1-A8:klp5* is viable (but very sick) at room temperature and lethal at the non-permissive 37°C [33]. Our numerous attempts to construct the triple deletion-inactivation mutant *cut7.24^{ts}:dam1-A8:klp5* proved unsuccessful, most likely because *dam1-A8:klp5* itself is very sick even at permissive temperature [33]. Nevertheless, the *dam1-A8:klp5* double-mutant exhibits longer metaphase spindles compared to the individual mutant *dam1* and *klp5* or to the wildtype cells (Fig. S2B, S2C), consistent with the tug-of-war analogy. In the course of this study, we also discovered that temperature-sensitivity is tenuous. It is known that different temperature-sensitive alleles of *cut7⁺* have different inactivation penetration, e.g., *cut7.24^{ts}* is lethal, but *cut7.21^{ts}* and *cut7.23^{ts}* are not lethal (but very sick) at the non-permissive temperature [7]. Further, we find that the allele *cut7.24^{ts}*, when tagged with GFP, is no longer lethal at 37°C (Fig. S2A), presumably because GFP confers added stability to the *cut7.24^{ts}* gene product. This implies that creating a fast-acting, strongly penetrant, temperature-sensitive mutant allele requires some serendipity.

We next measured the metaphase spindle lengths after the removal of different combinations of antagonist forces. We found that for all combinations of double-deletion, the removal of

antagonist forces lead to metaphase spindle lengths which are similar to wildtype and different from individual deletion (Fig. 2D). Indeed, *klp5* :*ase1* has a metaphase length of $3.17 \pm 0.78 \mu\text{m}$ and *dam1* :*ase1* has a metaphase length of $2.65 \pm 0.31 \mu\text{m}$, values significantly different from individual deletions (Fig. 2D). Interesting, only the double-deletion *dam1* :*ase1* appeared to rescue the prophase-metaphase duration (Fig. 2F), but *klp5* :*ase1* showed similar prophase-metaphase delay as individual *klp5* deletion. Further, while metaphase spindle length and some prophase-metaphase durations appeared rescued in the double-deletion, the prophase velocities are only partially rescued for *dam1* :*ase1* (Fig. S2E, S2F), and not rescued at all for *klp5* :*ase1* (Fig. S2D, S2F). At the non-permissive temperature of 35°C , *cut7.24^{ts} : klp6* has a metaphase length of $2.88 \pm 1.04 \mu\text{m}$ and *cut7.24^{ts} : dam1* has a metaphase length of $2.65 \pm 0.68 \mu\text{m}$, values closer to the wildtype $2.16 \pm 0.50 \mu\text{m}$ than the individual deletion or inhibition (Fig. 2E). These results are consistent with the role of *cut7p* as an active pushing force producer, *klp5/6p* as an active pulling force transducer, *dam1p* as a passive pulling force transducer, and *ase1p* as a passive pulling force resistor. Antagonism between *cut7p* and *ase1p* against *klp5/6p* and *dam1p* results in a steady-state spindle length.

Removal of any single or a combination of force contributors will result in a new steady-state length. The transition from one length to a new length can be smooth (stable) or not smooth (unstable) depending on the state of antagonism. In general, active-active antagonism, such as found in *dam1* :*ase1*, tend to produce a stable transition, represented by the smooth length vs. time trace (Fig. S2E). In contrast, an active-passive antagonism, such as found in *klp5* :*ase1*, tend to produce an unstable transition, represented by strong variations in the length vs. time trace (Fig. S2D). Further, stable spindle transition, such as found in *dam1* :*ase1* (Fig. S2E), may enable efficient kinetochore-to-MT attachment, which will result in seemingly normal (or rescued) prophase-metaphase duration (Fig. 2F). In contrast, unstable spindle transition, such as found in *klp5* :*ase1* (Fig. S2D), will be inefficient at kinetochore-to-MT attachment, which will result in a higher prophase-metaphase duration (Fig. 2F), likely due to the activation of the SAC.

Rescuing metaphase spindle length rescues chromosome segregation defects only when kinetochore-to-MT attachment is not severely compromised

The fidelity of chromosome segregation critically depends on the proper kinetochore-to-MT attachment occurring at metaphase [29–32]. There is a correlation between mutations which change the metaphase steady-state spindle length and chromosome segregation defects [19, 34, 35]. We asked if the apparent rescue of metaphase spindle length seen in the removal of antagonist forces would also rescue chromosome segregation defects. We performed live-cell imaging on mutant strains expressing mCherry-*atb2p* and CEN1-GFP (marker for the centromere/kinetochore of chromosome 1) [36]. We observed three distinct kinetochore behaviors: “normal”, where the sister kinetochores separate to opposite poles at anaphase; “lagging”, where the sister kinetochores are mis-segregated to one pole, but ultimately are corrected and separated to opposite poles; and “mis-segregation”, where sister kinetochores stayed at one pole and never separate to opposite poles (Fig. 3A). Compared to individual *klp5* (or *klp6*), both *klp5* :*ase1* and *klp6* :*cut7.24^{ts}* showed significant increase in normal kinetochore separation and decrease in lagging or mis-segregation of chromosome

(Fig. 3B, 3C). In contrast, compared to individual *dam1*, *dam1 :ase1* showed no significant change in kinetochore behavior (Fig. 3D); while *dam1 :cut7.24^{ts}* showed a decrease in normal kinetochore separation and an increase in kinetochore mis-segregation (Fig. 3E). We conclude that proper kinetochore-to-MT attachment is more important than spindle length regulation for proper chromosome segregation. The artificial minichromosome loss assay also yielded similar conclusions (Fig. S3A–B).

Transient spindle shrinkage precedes proper chromosome segregation in the *klp5 :ase1* and *klp6 :cut7.24^{ts}* mutants

How do the *klp5 :ase1* and *klp6 :cut7.24^{ts}* double-mutants, which have metaphase spindle lengths similar to wildtype cells, rescue chromosome segregation defects? In live-cell imaging of spindle and kinetochore dynamics, we observed that in all instances where the sister kinetochores are properly separated, approximately ~2 min prior to kinetochore separation at anaphase the spindle length exhibited a transient length decrease before resuming elongation (Fig. 4A–D). The start of resumed elongation coincided with kinetochore separation to opposite poles (Fig. 4A–D). This spindle length decrease only occurs in the double-mutants *klp5 :ase1* and *klp6 :cut7.24^{ts}*, but not the individual mutant *klp5* or *klp6*. We conclude that there is a correlation between transient spindle shrinkage and proper chromosome segregation in the *klp5 :ase1* and *klp6 :cut7.24^{ts}* double-mutants.

Interestingly, the transient spindle shrinkage prior to kinetochore separation was not observed in *dam1*, *dam1 :ase1*, nor *dam1 :cut7.24^{ts}* mutants (Fig. S4A–D). This result suggests that the spindle length decrease is not a general mechanism for rescuing chromosome segregation defects. Transient spindle shrinkage, due to instability in the balance of forces, may be a serendipitous mechanism enabling MTs to capture the kinetochores because MT plus ends are now closer to the kinetochores.

In summary, our current study tested the force-balance model in maintaining the steady-state metaphase spindle length in live-cell and using a microfluidic temperature-control device to tune on-off temperature-sensitive mutants during mitosis. While not exhaustive, we chose the key motors and MAPs that individually showed the most drastic changes to spindle length upon their deletion or inactivation. We have defined four categories in relation to force that exemplify the function of the proteins: 1) active outward force producer (kinesin-5 *cut7p*), 2) active inward force transducer (kinesin-8 *klp5/6p* heterodimer), 3) passive inward force transducer (kinetochore protein *dam1p*), and 4) passive inward force resistor (MT bundler *ase1p*). The force-balance, or tug-of-war, would be *cut7p* and *ase1p* against *klp5/6p* and *dam1p*. Clearly, our study is not exhaustive of all spindle proteins. There are hundreds of proteins which contribute to spindle length control [4], and thus, our approach of studying simultaneous double-deletion or inactivation can be applied systematically to all proteins implicated in metaphase spindle length control to define their individual relative contribution to chromosome segregation defects.

Experimental Procedures

Detailed descriptions are available in the Supplemental.

Supplementary Material

Refer to Web version on PubMed Central for supplementary material.

Acknowledgement

VS and CF designed and performed experiments, and analyzed data. VS and PTT wrote the paper. We thank the labs of J.R. McIntosh (University of Colorado), K. Gould (Vanderbilt University), T. Toda (CRUK), I. Hagan (Paterson Institute Cancer Research), D. McCollum (University of Massachusetts), and Y. Hiraoka (Kansai Advanced Research Center), and the Japan National BioResource Project for generously providing reagents. We thank Judite Costa and Guilhem Velve-Casquillas for helpful technical advice and discussion. This work is supported by grants from the NIH and ANR.

References

- Dumont S, Mitchison TJ. Force and length in the mitotic spindle. *Curr Biol.* 2009; 19:R749–R761. [PubMed: 19906577]
- Goshima G, Scholey JM. Control of mitotic spindle length. *Annu Rev Cell Dev Biol.* 2010; 26:21–57. [PubMed: 20604709]
- Mogilner A, Craig E. Towards a quantitative understanding of mitotic spindle assembly and mechanics. *Journal of cell science.* 2009; 123:3435–3445. [PubMed: 20930139]
- Goshima G, Wollman R, Stuurman N, Scholey JM, Vale RD. Length control of the metaphase spindle. *Curr Biol.* 2005; 15:1979–1988. [PubMed: 16303556]
- Saunders WS, Hoyt MA. Kinesin-related proteins required for structural integrity of the mitotic spindle. *Cell.* 1992; 70:451–458. [PubMed: 1643659]
- Tanenbaum ME, Macurek L, Janssen A, Geers EF, Alvarez-Fernandez M, Medema RH. Kif15 cooperates with eg5 to promote bipolar spindle assembly. *Curr Biol.* 2009; 19:1703–1711. [PubMed: 19818618]
- Troxell CL, Swezy MA, West RR, Reed KD, Carson BD, Pidoux AL, Cande WZ, McIntosh JR. pkl1(+) and klp2(+): Two kinesins of the Kar3 subfamily in fission yeast perform different functions in both mitosis and meiosis. *Molecular biology of the cell.* 2001; 12:3476–3488. [PubMed: 11694582]
- Nabeshima K, Nakagawa T, Straight AF, Murray A, Chikashige Y, Yamashita YM, Hiraoka Y, Yanagida M. Dynamics of centromeres during metaphase-anaphase transition in fission yeast: Dis1 is implicated in force balance in metaphase bipolar spindle. *Molecular biology of the cell.* 1998; 9:3211–3225. [PubMed: 9802907]
- Fu C, Ward JJ, Loiodice I, Velve-Casquillas G, Nedelec FJ, Tran PT. Phospho-regulated interaction between kinesin-6 Klp9p and microtubule bundler Ase1p promotes spindle elongation. *Developmental cell.* 2009; 17:257–267. [PubMed: 19686686]
- Decottignies A, Zarzov P, Nurse P. In vivo localisation of fission yeast cyclin-dependent kinase cdc2p and cyclin B cdc13p during mitosis and meiosis. *Journal of cell science.* 2001; 114:2627–2640. [PubMed: 11683390]
- Tatebe H, Goshima G, Takeda K, Nakagawa T, Kinoshita K, Yanagida M. Fission yeast living mitosis visualized by GFP-tagged gene products. *Micron.* 2001; 32:67–74. [PubMed: 10900382]
- Garcia MA, Koonrugsa N, Toda T. Two kinesin-like Kin I family proteins in fission yeast regulate the establishment of metaphase and the onset of anaphase A. *Curr Biol.* 2002; 12:610–621. [PubMed: 11967147]
- West RR, Malmstrom T, McIntosh JR. Kinesins klp5(+) and klp6(+) are required for normal chromosome movement in mitosis. *Journal of cell science.* 2002; 115:931–940. [PubMed: 11870212]
- Erent M, Drummond DR, Cross RA. S. pombe kinesins-8 promote both nucleation and catastrophe of microtubules. *PLoS one.* 2012; 7:e30738. [PubMed: 22363481]

15. Grissom PM, Fiedler T, Grishchuk EL, Nicastro D, West RR, McIntosh JR. Kinesin-8 from fission yeast: a heterodimeric, plus-end-directed motor that can couple microtubule depolymerization to cargo movement. *Molecular biology of the cell*. 2009; 20:963–972. [PubMed: 19037096]
16. Grishchuk EL, Efremov AK, Volkov VA, Spiridonov IS, Gudimchuk N, Westermann S, Drubin D, Barnes G, McIntosh JR, Ataullakhanov FI. The Dam1 ring binds microtubules strongly enough to be a processive as well as energy-efficient coupler for chromosome motion. *Proc Natl Acad Sci U S A*. 2008; 105:15423–15428. [PubMed: 18824692]
17. Grishchuk EL, Spiridonov IS, Volkov VA, Efremov A, Westermann S, Drubin D, Barnes G, Ataullakhanov FI, McIntosh JR. Different assemblies of the DAM1 complex follow shortening microtubules by distinct mechanisms. *Proc Natl Acad Sci U S A*. 2008; 105:6918–6923. [PubMed: 18460602]
18. Loiodice I, Staub J, Setty TG, Nguyen NP, Paoletti A, Tran PT. Ase1p organizes antiparallel microtubule arrays during interphase and mitosis in fission yeast. *Molecular biology of the cell*. 2005; 16:1756–1768. [PubMed: 15689489]
19. Yamashita A, Sato M, Fujita A, Yamamoto M, Toda T. The roles of fission yeast ase1 in mitotic cell division, meiotic nuclear oscillation, and cytokinesis checkpoint signaling. *Molecular biology of the cell*. 2005; 16:1378–1395. [PubMed: 15647375]
20. Subramanian R, Wilson-Kubalek EM, Arthur CP, Bick MJ, Campbell EA, Darst SA, Milligan RA, Kapoor TM. Insights into antiparallel microtubule crosslinking by PRC1, a conserved nonmotor microtubule binding protein. *Cell*. 2010; 142:433–443. [PubMed: 20691902]
21. Grishchuk EL, Spiridonov IS, McIntosh JR. Mitotic chromosome biorientation in fission yeast is enhanced by dynein and a minus-end-directed, kinesin-like protein. *Molecular biology of the cell*. 2007; 18:2216–2225. [PubMed: 17409356]
22. Olmsted ZT, Riehlman TD, Branca CN, Colliver AG, Cruz LO, Paluh JL. Kinesin-14 Pkl1 targets gamma-tubulin for release from the gamma-tubulin ring complex (gamma-TuRC). *Cell cycle (Georgetown, Tex)*. 2013; 12:842–848.
23. Hagan I, Yanagida M. Kinesin-related cut7 protein associates with mitotic and meiotic spindles in fission yeast. *Nature*. 1992; 356:74–76. [PubMed: 1538784]
24. Velve Casquillas G, Fu C, Le Berre M, Cramer J, Meance S, Plecis A, Baigl D, Greffet JJ, Chen Y, Piel M, et al. Fast microfluidic temperature control for high resolution live cell imaging. *Lab Chip*. 2011; 11:484–489. [PubMed: 21103458]
25. Blangy A, Lane HA, d'Herin P, Harper M, Kress M, Nigg EA. Phosphorylation by p34cdc2 regulates spindle association of human Eg5, a kinesin-related motor essential for bipolar spindle formation in vivo. *Cell*. 1995; 83:1159–1169. [PubMed: 8548803]
26. Kapoor TM, Mayer TU, Coughlin ML, Mitchison TJ. Probing spindle assembly mechanisms with monastrol, a small molecule inhibitor of the mitotic kinesin, Eg5. *The Journal of cell biology*. 2000; 150:975–988. [PubMed: 10973989]
27. Saunders AM, Powers J, Strome S, Saxton WM. Kinesin-5 acts as a brake in anaphase spindle elongation. *Curr Biol*. 2007; 17:R453–R454. [PubMed: 17580072]
28. Kollu S, Bakhom SF, Compton DA. Interplay of microtubule dynamics and sliding during bipolar spindle formation in mammalian cells. *Curr Biol*. 2009; 19:2108–2113. [PubMed: 19931454]
29. Lara-Gonzalez P, Westhorpe FG, Taylor SS. The spindle assembly checkpoint. *Curr Biol*. 2012; 22:R966–R980. [PubMed: 23174302]
30. Musacchio A. Spindle assembly checkpoint: the third decade. *Philosophical transactions of the Royal Society of London*. 2011; 366:3595–3604. [PubMed: 22084386]
31. Musacchio A, Salmon ED. The spindle-assembly checkpoint in space and time. *Nature reviews*. 2007; 8:379–393.
32. Vleugel M, Hoogendoorn E, Snel B, Kops GJ. Evolution and function of the mitotic checkpoint. *Developmental cell*. 2012; 23:239–250. [PubMed: 22898774]
33. Griffiths K, Masuda H, Dhut S, Toda T. Fission yeast dam1-A8 mutant is resistant to and rescued by an anti-microtubule agent. *Biochemical and biophysical research communications*. 2008; 368:670–676. [PubMed: 18262494]

34. Sanchez-Perez I, Renwick SJ, Crawley K, Karig I, Buck V, Meadows JC, Franco-Sanchez A, Fleig U, Toda T, Millar JB. The DASH complex and Klp5/Klp6 kinesin coordinate bipolar chromosome attachment in fission yeast. *The EMBO journal*. 2005; 24:2931–2943. [PubMed: 16079915]
35. West RR, Malmstrom T, Troxell CL, McIntosh JR. Two related kinesins, klp5+ and klp6+, foster microtubule disassembly and are required for meiosis in fission yeast. *Molecular biology of the cell*. 2001; 12:3919–3932. [PubMed: 11739790]
36. Yamamoto A, Hiraoka Y. Monopolar spindle attachment of sister chromatids is ensured by two distinct mechanisms at the first meiotic division in fission yeast. *The EMBO journal*. 2003; 22:2284–2296. [PubMed: 12727894]

Highlights

1. The force-balance model of metaphase spindle length control is tested.
2. Microfluidic temperature-control enables studies of antagonistic motors and MAPs.
3. Kinesin-5 *cut7p* and MT bundler *ase1p* contribute to outward pushing forces.
4. Kinetochores proteins kinesin-8 *klp5/6p* and *dam1p* contribute to inward pulling forces.

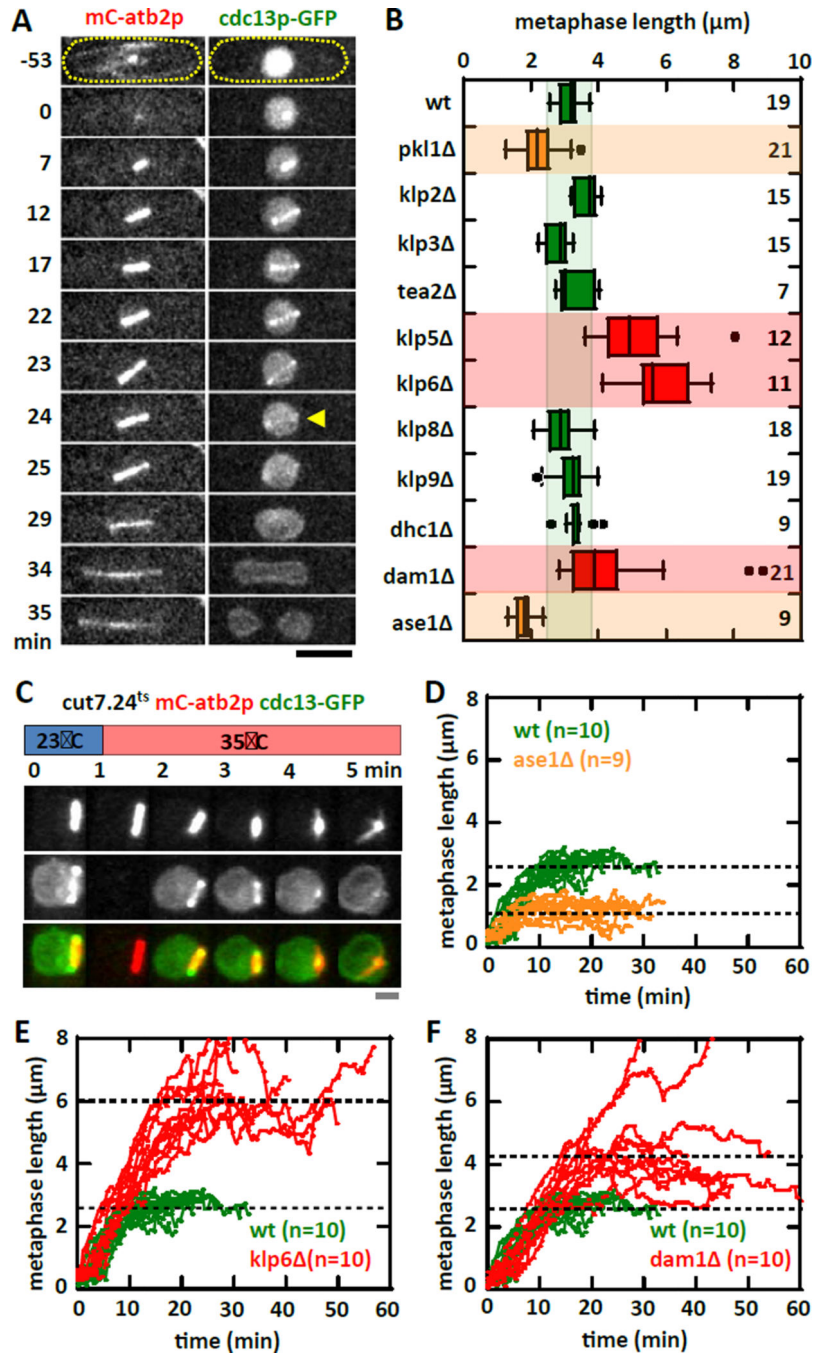


Figure 1. Motors and MAPs contribute to metaphase spindle length force-balance mechanism
(A) Time-lapse images of a wildtype cell expressing mCherry-atb2p (tubulin) and cdc13p-GFP (cyclin) through mitosis. cdc13p is degraded from the spindle at the metaphase to anaphase transition (yellow arrow), marking precisely the final metaphase spindle length. The cdc13p-GFP marker is used in the screen for motors and MAPs affecting metaphase spindle length (see Fig. 1B). Bar, 5 μ m.
(B) Targeted screen of fission yeast motors and selective MAPs for defects in metaphase spindle length at room temperature (23 $^{\circ}$ C). Box plot shows spindle lengths - wildtype (3.1 \pm

0.3 μm), *pk11* ($2.0 \pm 0.4 \mu\text{m}$, $p < 10^{-4}$), *klp2* ($3.6 \pm 0.3 \mu\text{m}$, $p < 10^{-4}$), *klp3* ($2.8 \pm 0.4 \mu\text{m}$, $p = 0.1$), *tea2* ($3.3 \pm 0.5 \mu\text{m}$, $p = 0.3$), *klp5* ($5.3 \pm 1.2 \mu\text{m}$, $p < 10^{-4}$), *klp6* ($6.3 \pm 1.6 \mu\text{m}$, $p < 10^{-4}$), *klp8* ($2.9 \pm 0.5 \mu\text{m}$, $p = 0.4$), *klp9* ($3.4 \pm 0.4 \mu\text{m}$, $p = 0.6$), *dhc* ($3.4 \pm 0.4 \mu\text{m}$, $p = 0.1$), *dam1* ($4.4 \pm 1.6 \mu\text{m}$, $p < 10^{-2}$), and *ase1* ($1.8 \pm 0.3 \mu\text{m}$, $p < 10^{-7}$).

(C) Temperature shift experiment of kinesin-5 cut7.24^{ts} cells expressing mCherry-*atb2p* and *cdc13p*-GFP. Within 1 min of shifting to the non-permissive temperature of 35°C, the metaphase spindle exhibits spindle shortening and collapse, ultimately becoming a monopolar spindle. Note: The blank image at time 1-min in the *cdc13p*-GFP channel was due to thermal expansion of the coverslip causing an out-of-focus image, which was corrected in subsequent frames. Bar, 1 μm .

(D) Comparative plot of spindle length versus time of wildtype (green) and *ase1* (*organe*) cells. Shown are pole-to-pole distances measured from prophase to the metaphase-anaphase transition. Wildtype metaphase spindles plateau at ~3 μm length. In contrast, *ase1* metaphase spindles plateau at ~2 μm length.

(E) Comparative plot of spindle length versus time of wildtype (green) and *klp6* (red) cells. In contrast to wildtype, *klp6* metaphase spindles plateau at ~6 μm length.

(F) Comparative plot of spindle length versus time of wildtype (green) and *dam1* (red) cells. In contrast to wildtype, *dam1* metaphase spindles plateau at ~4 μm length.

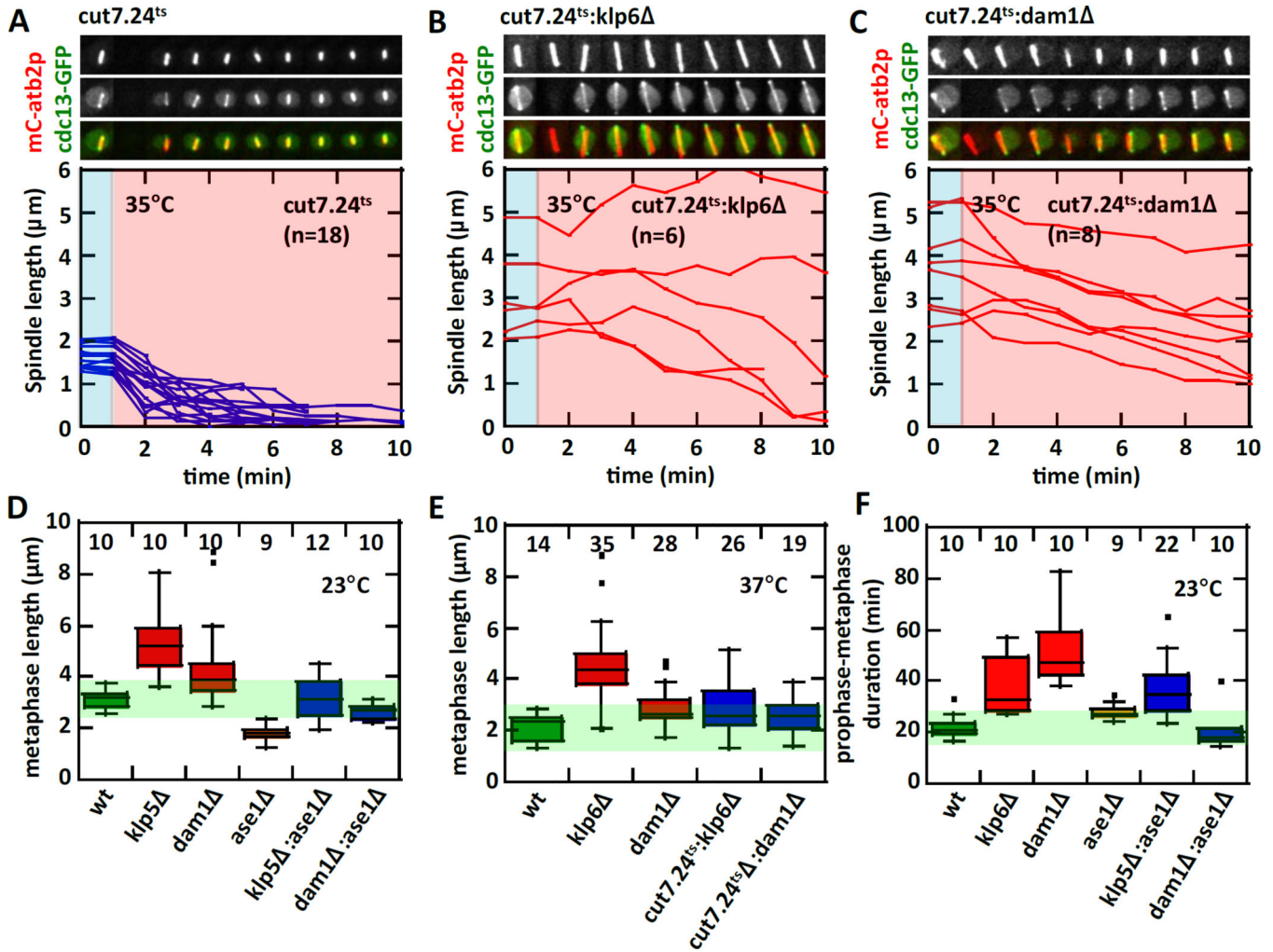


Figure 2. Removing antagonistic spindle forces rescues metaphase spindle length defects
 (A) Temperature shift experiment of *cut7.24^{ts}* cells expressing mCherry-atb2p and cdc13p-GFP. The accompanying plot of spindle length versus time shows that all *cut7.24^{ts}* metaphase spindles shorten and collapse within ~3–4 min at the non-permissive temperature of 35°C.

(B) Temperature shift experiment of *cut7.24^{ts}:klp6Δ* double-mutant cells. The double-mutant cells do not exhibit the fast spindle collapse as seen in *cut7.24^{ts}* alone (see Fig. 2A). The metaphase spindles maintain transiently stable lengths during the 10 min of observation at the non-permissive temperature.

(C) Temperature shift experiment of *cut7.24^{ts}:dam1Δ* double-mutant cells. The double-mutant cells do not exhibit the fast spindle collapse as seen in *cut7.24^{ts}* alone. The metaphase spindles slowly shorten during the 10 min of observation at the non-permissive temperature.

(D) Box plot shows metaphase spindle lengths measured at 23°C. Individual mutants have defective spindle length. Metaphase spindle lengths - wildtype, *klp5Δ*, *dam1Δ*, and *ase1Δ* are reported in Fig. 1B. In contrast, antagonistic double-mutants rescue the spindle length defects of the single mutants. Metaphase spindle length of *klp5Δ:ase1Δ* ($3.2 \pm 0.8 \mu\text{m}$) is

similar to wildtype ($p=0.8$), and $dam1 :ase1$ ($2.6 \pm 0.3 \mu\text{m}$) is between $dam1$ ($p<10^{-4}$) and $ase1$ ($p<10^{-4}$).

(E) Box plot shows metaphase spindle lengths measured at 37°C . Individual mutants have defective spindle length. Metaphase spindle lengths - wildtype ($2.2 \pm 0.5 \mu\text{m}$), $cut7.24^{ts}$ ($1.5 \pm 0.4 \mu\text{m}$, $p<0.004$), $klp6$ ($4.6 \pm 1.6 \mu\text{m}$, $p<10^{-10}$), and $dam1$ ($2.9 \pm 0.7 \mu\text{m}$, $p<10^{-3}$). In contrast, antagonistic double-mutants rescue the spindle length defects of the single mutants. Metaphase spindle length of $cut7.24^{ts}:klp6$ ($2.9 \pm 1.0 \mu\text{m}$) is between $cut7.24^{ts}$ ($p<10^{-5}$) and $klp6$ ($p<10^{-5}$), and $cut7.24^{ts}:dam1$ ($2.7 \pm 0.7 \mu\text{m}$) is between $cut7.24^{ts}$ ($p<10^{-4}$) and $dam1$ ($p=0.2$).

(F) Box plot shows prophase-metaphase duration measured at 23°C . Individual mutants have prolonged prophase-metaphase durations. Durations - wildtype ($22 \pm 5 \text{ min}$), $klp6$ ($38 \pm 11 \text{ min}$, $p<0.002$), $dam1$ ($52 \pm 13 \text{ min}$, $p<10^{-4}$), and $ase1$ ($28 \pm 3 \text{ min}$, $p<0.007$). In contrast, some antagonistic double-mutants rescue prophase-metaphase duration defects of the single mutants. Durations - $dam1 :ase1$ ($21 \pm 7 \text{ min}$) is similar to wildtype ($p=0.5$), and $klp5 :ase1$ ($37 \pm 11 \text{ min}$) is similar to $klp6$ ($p=0.8$).

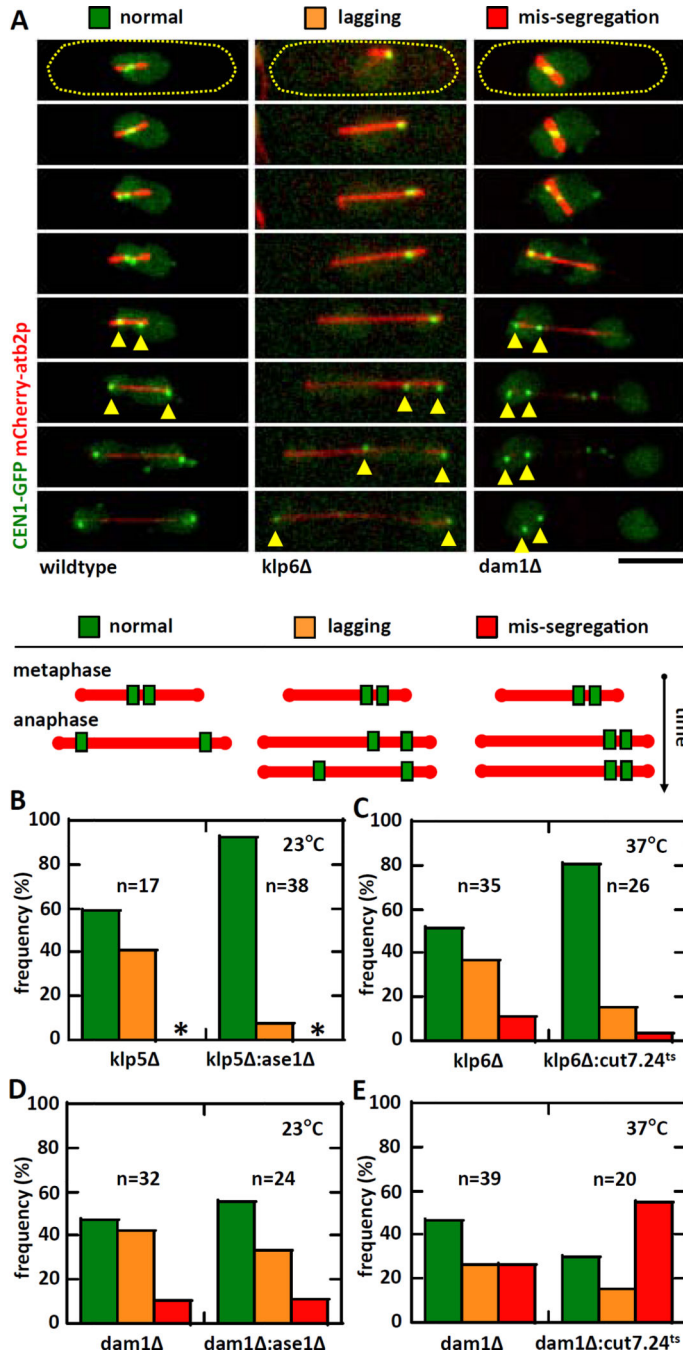


Figure 3. Rescuing metaphase spindle length defects partially rescues chromosome segregation defects

(A) Time-lapse images of mitotic cells expressing mCherry-atb2p (tubulin) and CEN1-GFP (centromere of chromosome 1). We defined the behavior of chromosomes as: normal – sister centromeres separate equally to daughter cells at anaphase; lagging – sister centromeres show delayed separation to daughter cells at anaphase (yellow arrow heads); mis-segregation – sister centromeres stay in one daughter cell at the completion of mitosis (orange arrow heads).

(B) Plot shows frequency comparison of chromosome behavior between *klp5* and *klp5 :ase1* at 23°C. No chromosome mis-segregation is observed for these strains (asterisk). The *klp5 :ase1* strain shows ~90% normal chromosome segregation compared to ~60% for *klp5* alone ($p < 10^{-34}$). Note: wildtype cells have 100% normal chromosome segregation.

(C) Plot shows frequency comparison of chromosome behavior between *klp6* and *cut7.24^{ts}:klp6* at 37°C. The *cut7.24^{ts}:klp6* strain shows ~80% normal chromosome segregation compared to ~50% for *klp6* alone ($p < 10^{-9}$).

(D) Plot shows frequency comparison of chromosome behavior between *dam1* and *dam1 :ase1* cells at 23°C. No significant changes in the behavior of chromosomes was observed in the double-mutant compared to single-mutant ($p = 0.2$).

(E) Plot shows frequency comparison of chromosome behavior between *dam1* and *dam1 :cut7.24^{ts}* at 37°C. In deed, the *dam1 :cut7.24^{ts}* strain shows ~55% of mis-segregation compared to ~25% for *dam1* alone ($p < 10^{-9}$).

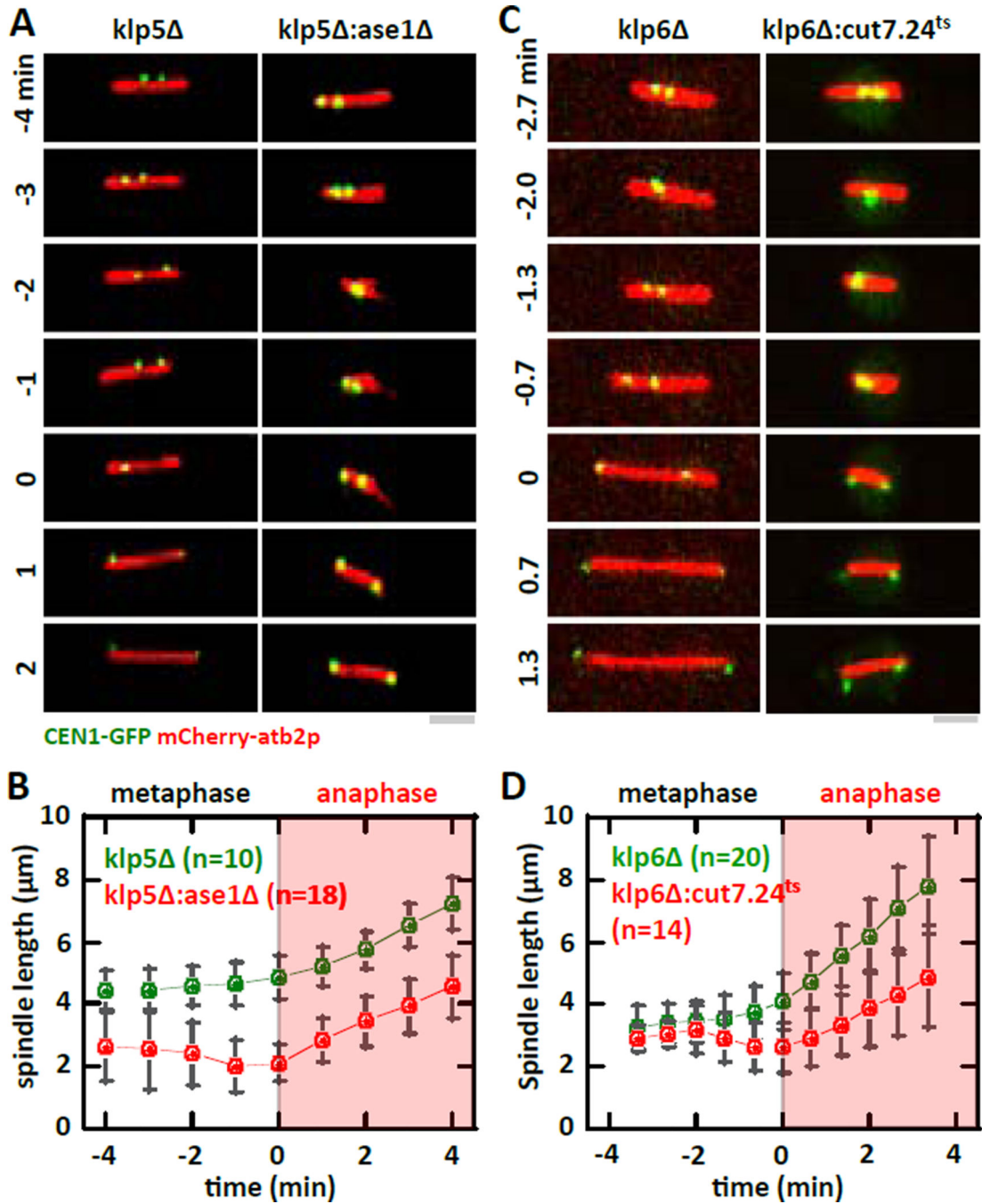


Figure 4. Transient abrupt metaphase spindle length decrease precedes proper chromosome segregation

(A) Time-lapse images of *klp5Δ* and *klp5Δ:ase1Δ* mitotic cells expressing mCherry-atb2p and CEN1-GFP at 23°C. Time 0 represents the transition from metaphase to anaphase A where sister kinetochores are observed to separate to opposite poles. Whereas the metaphase spindle exhibits sustained elongation during the metaphase to anaphase transition in *klp5Δ* cells, *klp5Δ:ase1Δ* cells show transient spindle shrinkage prior to the metaphase to anaphase transition. Bar, 1 μm.

(B) Comparative spindle length versus time plot of *klp5* (green) and *klp5 :ase1* (red) cells. Pole-to-pole distance was measured 4 minute before and 4 minutes after cells exhibit kinetochore separation to opposite poles. At -2 min, the spindle length of the double-mutant exhibits a transient shrinkage.

(C) Time-lapse images of *klp6* and *klp6 :cut7.24^{ts}* mitotic cells expressing mCherry-atb2p and CEN1-GFP at 37°C. Time 0 represents the transition from metaphase to anaphase A where sister kinetochores are observed to separate to opposite poles. Whereas the metaphase spindle exhibits sustained elongation during the metaphase to anaphase transition in *klp6* cells, *klp6 :cut7.24^{ts}* cells show transient spindle shrinkage prior to the metaphase to anaphase transition. Bar, 1 μ m.

(D) Comparative spindle length versus time plot of *klp6* (green) and *klp6 :cut7.24^{ts}* (red) cells. Pole-to-pole distance was measured 3.5 minute before and 3.5 minutes after cells exhibit kinetochore separation to opposite poles. At -2 min, the spindle length of the double-mutant exhibits a transient shrinkage.